

# Synthesis, Characterization and Biological Activity of Neomycin Sulphate Complexes

Mamdouh S. Masoud, Galila A. Yacout, Samir K. El-Saadany, Bassant A. Abd-El-Khalek\*

**Abstract:** - A series of transition metals neomycin complexes having the formula  $[M(\text{Neom})(\text{H}_2\text{O})_m \text{Cl}_n] \cdot x\text{H}_2\text{O} \cdot 3\text{SO}_4$  were prepared; where M (metal) = Vanadium V(II), Chromium Cr(III), Iron Fe(III), Cobalt Co(II), Nickel Ni(II), Copper Cu(II), Zinc Zn(II), Cadmium Cd(II) or Palladium Pd(II) ions, Neom= neomycin,  $m=1-4$ ,  $n=0,1$  and  $x= 3-5$ . The complexes have been characterized by elemental analysis, magnetic moment measurements, IR spectra, electronic spectra, ESR spectra and thermal analyses. IR spectra indicated that the bonding between neomycin and transition metal ions takes place through M-O bonds. Neomycin can react with metal ions as dianionic bidentate ligand through  $\text{H}^+$  ion displacement from 2 OH alcoholic groups. The thermodynamic activation parameters such as: energy of activation  $\Delta E^*$ , enthalpy of activation  $\Delta H^*$ , entropy of activation  $\Delta S^*$  and free energy of activation  $\Delta G^*$  were calculated from the Thermogravimetric (TG) curves for complexes. Some statistical studies were done using computer programs to give extra spotlights on the bonding properties of these compounds. Biological screening for neomycin and some of its synthesized complexes involving antimicrobial (antibacterial, antifungal) and antioxidant were done.

**Keywords:** - Neomycin sulphate, Metal complexes, Analysis, Spectra, Molecular modeling, Biological activity.

## 1 INTRODUCTION:-

Medical inorganic chemistry is becoming an important area of research due to the demand for new biologically active compounds. Inorganic compounds especially transition metals have played an important role in the development of new metal based drugs. Various investigations have reported that binding of a drug to a metallo element increases its effectiveness and the complex possesses even more healing properties than the parent drug [1]. Transition metal complexes are also important in photochemistry, catalysis, materials synthesis, and biological systems. They display diverse chemical, optical and magnetic properties [2].

Most antibiotics of clinical relevance are derivatives of naturally occurring microbial products. The aminoglycosides are a class of clinically important antibiotics that have been widely used to treat chronic bacterial infections of the heart, lung and urinary tract [3].

The chemical structures of aminoglycosides are similar. All of them are organic alkalis with a high dissociation and low lipid diffusion, and do not easily transport across membranes. They consist of amino sugar connected by a glycosidic bond to 2-deoxystreptamine which connected by another glycosidic bond to amino sugar.

Neomycin sulphate, Figure 1, is a bactericidal aminoglycoside antibiotic containing two or more aminosugars connected by glycosidic bonds.

- Mamdouh S. Masoud: - Prof. of Inorganic and Analytical Chemistry, Chemistry Department, Faculty of Science, Alexandria University, Alexandria, Egypt.
- Galila A. Yacout: - Prof. of Biochemistry, Biochemistry Department, Faculty of Science, Alexandria University, Alexandria, Egypt.
- Samir K. El-Saadany: - Prof. of Organic Chemistry, Chemistry Department, Faculty of Science, Alexandria University, Alexandria, Egypt.
- Corresponding author\*:-
- Bassant A. Abd-El-Khalek: - is currently pursuing PhD degree program in Chemistry, Chemistry Department, Faculty of Science, Alexandria University, Alexandria, Egypt. E-mail: bassantahmed391@yahoo.com.

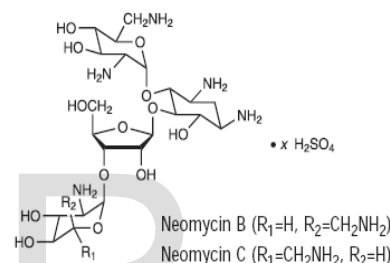


Fig. 1. Chemical structure of Neomycin Sulphate.

It is a mixture of neomycin A (neamine), neomycin B (framycetin), neomycin C, and a few minor compounds found in much lower quantities. Neomycin sulphate is white powder, odorless, melting point  $>187$  ( $^{\circ}\text{C}$ ) and soluble in water, ethanol, methanol, isopropyl, isoamyl alcohol and benzene but insoluble in acetone, chloroform and ether. Boiling/Freezing Points ( $^{\circ}\text{C}$ ) are approximately same as water.

Neomycin sulphate has excellent activity against gram-negative bacteria, and has partial activity against gram-positive bacteria [4], [5].

Some studies were reported about the solid complexes of neomycin with transition metal (II) ions. A series of polymeric  $[M(\text{Neom})(\text{H}_2\text{O})_X]_n$  complexes have been prepared; where  $M= \text{Co(II)}$ ,  $\text{Ni(II)}$ ,  $\text{Cu(II)}$  or  $\text{Zn(II)}$  ions, Neom= neomycin and  $x=2-4$  [6].

It is aimed in the present work to synthesize Vanadium, Chromium, Iron, Cobalt, Nickel, Copper, Zinc, Cadmium and Palladium complexes with neomycin. The complexes have been characterized by elemental analysis, magnetic moment measurements, Infra-Red spectra, electronic spectra, Electron Spin Resonance spectrum of copper complex and thermal analyses. Some statistical studies were done using computer programs to give extra spotlights on the bonding properties of these compounds (bond lengths, bond angles, dihedral angles and charges). Moreover, biological screening for some of neomycin complexes involving antimicrobial (antibacterial, antifungal) and antioxidant were done and compared with the activity of neomycin itself.

## 2 EXPERIMENTAL:-

Neomycin sulphate was supplied by Memphies and Squibb companies, whereas all compounds used in the present investigation were Aldrich or BDH pure grade chemicals.

### 2.1 Synthesis of the complexes:-

All the complexes were prepared in a similar manner. The required weight of transition metal chloride salt was dissolved in water and mixed with the required weight of neomycin dissolved in water. The reaction mixture was heated for 15 minutes, then cooled where a precipitate was formed, filtered then dried in an oven at ~ 90°C. The products are formed with the molar ratio 1:1 for all complexes. The analytical data of the studied compounds are represented in Table 1.

TABLE 1: COLOR, ELEMENTAL ANALYSIS ROOM TEMPERATURE (298°C) EFFECTIVE MAGNETIC MOMENT VALUES, λ<sub>MAX</sub> (NM) AND GEOMETRIES OF THE COMPLEXES.

Complex	M.wt	Color	Calculated/(Found)%						λ <sub>max</sub> (nm)	μ <sub>eff</sub> (298°K)	Geometry
			M	C	H	N	Cl	SO <sub>4</sub>			
[C <sub>21</sub> H <sub>29</sub> N <sub>5</sub> O <sub>10</sub> .V.4H <sub>2</sub> O](SO <sub>4</sub> ) <sub>3</sub> .H <sub>2</sub> O	1101	Dark green	4.9 (4.5)	26.8 (27.23)	5.6 (6.12)	8.2 (8.61)	----	27.9 (26.7)	200,450,800	4.21	O <sub>h</sub>
[C <sub>21</sub> H <sub>29</sub> N <sub>5</sub> O <sub>10</sub> .Cr.4H <sub>2</sub> O](SO <sub>4</sub> ) <sub>3</sub> .5H <sub>2</sub> O	1120	Pale green	5.0 (4.8)	27.2 (28.12)	5.5 (5.95)	8.1 (8.52)	----	27.8 (26.1)	330,440,610	5.12	O <sub>h</sub>
[C <sub>21</sub> H <sub>29</sub> N <sub>5</sub> O <sub>10</sub> .Fe.3H <sub>2</sub> O.Cl](SO <sub>4</sub> ) <sub>3</sub> .4H <sub>2</sub> O	1123.5	Dark brown	5.2 (5.1)	25.8 (26.21)	5.4 (5.85)	7.9 (8.42)	3.16 (3.32)	27 (25.9)	390,504	5.92	O <sub>h</sub>
[C <sub>21</sub> H <sub>29</sub> N <sub>5</sub> O <sub>10</sub> .Co.3H <sub>2</sub> O.Cl](SO <sub>4</sub> ) <sub>3</sub> .4H <sub>2</sub> O	1126.5	Rose	5.5 (5.3)	25.7 (26.11)	5.45 (5.88)	7.8 (8.31)	3.15 (3.31)	26.8 (25.3)	360,496,556	5.03	O <sub>h</sub>
[C <sub>21</sub> H <sub>29</sub> N <sub>5</sub> O <sub>10</sub> .Ni.H <sub>2</sub> O.Cl](SO <sub>4</sub> ) <sub>3</sub> .4H <sub>2</sub> O	1090	Pale green	5.4 (5.2)	25.9 (26.22)	5.3 (5.75)	7.6 (7.4)	3.26 (3.3)	26.7 (25)	660,568	4.12	T <sub>d</sub>
[C <sub>21</sub> H <sub>29</sub> N <sub>5</sub> O <sub>10</sub> .Cu.3H <sub>2</sub> O.Cl](SO <sub>4</sub> ) <sub>3</sub> .4H <sub>2</sub> O	1131	Dark blue	5.9 (5.7)	25.6 (25.91)	5.3 (5.75)	7.5 (7.3)	3.14 (3.2)	26.6 (26.1)	400,440,600,734	2.31	O <sub>h</sub>
[C <sub>21</sub> H <sub>29</sub> N <sub>5</sub> O <sub>10</sub> .Zn.H <sub>2</sub> O.Cl](SO <sub>4</sub> ) <sub>3</sub> .4H <sub>2</sub> O	1097	Pale yellow	6.3 (6.2)	26.5 (26.77)	5.2 (5.63)	8.0 (8.5)	3.24 (3.4)	27.6 (26.9)	560,600	Dia.	T <sub>d</sub>
[C <sub>21</sub> H <sub>29</sub> N <sub>5</sub> O <sub>10</sub> .Cd.H <sub>2</sub> O.Cl](SO <sub>4</sub> ) <sub>3</sub> .4H <sub>2</sub> O	1144	Pale yellow	9.9 (9.5)	24.5 (24.92)	5.1 (5.45)	7.5 (8.22)	3.1 (3.25)	25.6 (24.4)	500,610	Dia.	T <sub>d</sub>
[C <sub>21</sub> H <sub>29</sub> N <sub>5</sub> O <sub>10</sub> .Pd.2H <sub>2</sub> O](SO <sub>4</sub> ) <sub>3</sub> .4H <sub>2</sub> O	1120.4	Brown	10.1 (9.9)	28.3 (26.92)	5.1 (5.45)	7.9 (8.32)	----	27.5 (27.1)	480,635	Dia.	S.P

### 2.2 Methods of analyses:-

#### 2.2.1 Metal ion content:

The complexes were digested and decomposed with aqua regia. The process was done several times to ensure that all the organic matters were completely destroyed. The residue was dissolved in distilled water.

The free metal contents were determined by two methods. (i) Atomic absorption technique using Shimadzu- atomic absorption spectrophotometer, model 6650. (ii) complexometric titration procedure with standard EDTA solution [7]. Vanadium and palladium concentrations were determined by using Energy dispersive X-Ray Analysis (EDX) instrument at electron microscope unit, Faculty of Science, Alexandria University.

#### 2.2.2 Carbon (C), Hydrogen (H), Nitrogen (N), Chloride (Cl) and Sulphate (SO<sub>4</sub>) contents:

The analyses of C, H and N contents were performed at Micro analytical Unit, Faculty of Science, Cairo University. The analysis of chloride ion was performed by volhard method.

The sulphate content was determined by adding barium chloride which led to precipitate barium sulphate in a colloidal form of uniform size and this tendency is enhanced in presence of a sodium chloride, hydrochloric acid and glycerol. The absorbance of the barium sulfate formed is measured by a spectrophotometer at 420 nm and the sulphate ion concentration is determined by comparison of the reading with a standard curve.

### 2.3 Instruments and working procedures:-

#### 2.3.1 Electronic absorption spectra:

The spectral studies in solution were measured using Double beam Ultra violet-visible (UV-Visible) spectrophotometry (T70-UV/Vis) PG instruments covering the wavelength range 190-900 nm.

Measurements were performed at the central laboratory, Faculty of Science, Alexandria University. The complexes were measured in Nujol mull, following the method described by Lee, Griswold and Kleinberg [8].

#### 2.3.2 Infrared spectra:

The infrared spectra of the ligand and its metal complexes were taken in potassium bromide disc using Perkin Elmer spectrophotometer, Model 1430, covering frequency range of 200-4000 cm<sup>-1</sup>. Calibration of frequency reading was made with polystyrene film (1602 ± 1 cm<sup>-1</sup>). The instrument located at the central lab, Faculty of Science, Alexandria University, Alexandria, Egypt.

#### 2.3.3 Thermal analysis:

Thermal analysis (Differential thermal analysis, Thermo gravimetric and Differential Scanning Calorimetric) (DTA, TG and DSC) were performed using a Linseis STA PT-1000 under air atmosphere where, the rate of heating was 20°C/min. The instrument is located at the central laboratory, Faculty of Science, Alexandria University, Alexandria, Egypt.

#### 2.3.4 Magnetic susceptibility measurements:

Hg [Co (SCN) 4] was used for calibrating the Gouy tubes. Some of the complexes were measured using the Faraday method. Diamagnetic corrections were calculated from the data given by Figgis and Lewis [9].

#### 2.3.5 Electron spin resonance spectra (ESR):

X-band electron spin resonance spectra were recorded with a reflection spectrometer operating at (9.1-9.8) GHZ in a cylindrical resonance cavity with 100 KHZ modulation. The magnetic field was controlled with a (LMR Gauss meter). The g values were determined by comparison with 2, 2-diphenyl pyridyl hydrazone DPPH signal (g= 2.0037). The instrument is located at the central laboratory, Faculty of Science, Alexandria University.

#### 2.3.6 Antimicrobial activity:

To evaluate the effect of metal ions upon chelation, ligand and some of its synthesized complexes have been screened for their antimicrobial activities against two fungi (*Aspergillus fumigates* and *Candida albicans*), two gram positive bacteria (*Streptococcus pneumoniae* and *Bacillus subtilis*) and two gram negative bacteria (*Pseudomonas aeruginosa* and *Escherichia coli*). Screening tests regarding the inhibition zone were carried out by the well diffusion method [10].

#### 2.3.7 Antioxidant activity:

The stable radical 2, 2-diphenyl-1-picrylhydrazyl (DPPH) was used as a reagent for spectrophotometric assay. 200 μl serial concentrations of each sample (150, 300, 450, 600, 750, 900, 1000 mg) were mixed with 1 ml of DPPH (0.0025 g/ml in methanol), each separately. The mixture was shaken vigorously and then kept in dark for half an hour, the decrease in absorbance of each

mixture was measured spectro-photometrically at 517 nm. Blank was prepared, while vitamin E, a stable antioxidant, was used as a synthetic reference. The scavenging activity on the DPPH radical was performed [11], by measuring the absorbance at 517 nm until the reaction reached the steady state. The DPPH radical scavenging activity  $S\% = \frac{A_{\text{control}} - A_{\text{sample}}}{A_{\text{control}}} \times 100$ , where,  $A_{\text{control}}$  is the absorbance of the blank control solution and  $A_{\text{sample}}$  is the absorbance of the test sample [12].

### 2.4 Computer programs:-

The hyper chemistry version 8, ChemBioDraw Ultra 12.0 and ChemBio3D Ultra 12.0 computer programs have been used to molecular modeling of the ligand and its complexes and to give extra spotlights on the bonding properties of these compounds (bond lengths, bond angles, dihedral angles and charges).

## 3 RESULTS AND DISCUSSION:-

### 3.1 Elemental analysis:

On the basis of the analytical data, the metal neomycin complexes can be formulated as  $[M(\text{Neom})(\text{H}_2\text{O})_m \text{Cl}_n] \cdot x\text{H}_2\text{O} \cdot 3\text{SO}_4$ , where  $M = \text{V(II)}, \text{Cr(II)}, \text{Fe(III)}, \text{Co(II)}, \text{Ni(II)}, \text{Cu(II)}, \text{Zn(II)}, \text{Cd(II)}$  or  $\text{Pd(II)}$  ions, Neom= neomycin,  $m=1-4$ ,  $n=0,1$  and  $x=3-5$ .  $m=1$  in case of nickel, zinc and cadmium complexes, 2 in case of palladium complex, 3 in case of iron, cobalt and copper complexes and 4 in case of vanadium and chromium complexes.  $n=0$  in case of vanadium, chromium and palladium complexes and 1 in case of iron, cobalt, nickel, copper, zinc and cadmium complexes.  $x=3$  in case of vanadium complex, 4 in case of iron, cobalt, nickel, copper, zinc, cadmium and palladium complexes and 5 in case of chromium complex. This indicates that neomycin behaves as a dianionic bidentate ligand towards one metal ion.

### 3.2 Infrared spectra:

On comparing the infrared spectra of the prepared complexes with that of the free ligand; the following can be pointed out:-

- The spectra of the metal complexes exhibit a broad band at 3400-3500  $\text{cm}^{-1}$  corresponding to overlapping between two bands of  $\nu_{\text{NH}_2}$  &  $\nu_{\text{OH}}$  of coordinated water. This is confirmed by the presence of new band in the region 820-885  $\text{cm}^{-1}$ , assigned to the out of plane deformation vibrations of coordinated water [13].
- The spectra of the dehydrated complexes display interesting changes in comparison to that of free neomycin. The band located at 3395  $\text{cm}^{-1}$  in the spectra of ligand due to  $\nu_{\text{OH}}$  is shifted to lower wave number in the spectra of metal-neomycin complexes and with lower relative intensity suggesting coordination through oxygen atom in the prepared complexes.
- The appearance of the new band at 490-460  $\text{cm}^{-1}$  in the spectra of metal-neomycin complexes, which is absent in the spectra of free neomycin, can be assigned to  $\nu_{\text{M-O}}$ . This reveals that neomycin can react with metal ions as dianionic bidentate ligand through  $\text{H}^+$  ion displacement from 2 OH alcoholic groups.
- The band corresponding to  $\delta_{\text{OH}}$  at 1520  $\text{cm}^{-1}$  and  $\nu_{\text{C-OH}}$  at 1022  $\text{cm}^{-1}$  in the spectra of neomycin display an obvious decrease in intensity in the spectra of metal-neomycin complexes. The decreased relative intensity

can be ascribed to displacement of two protons from the 2 OH groups of neomycin by the metal ion leading to covalent bonding with the organic molecule.

- The band at 3150  $\text{cm}^{-1}$  due to  $\nu_{\text{NH}_2}$  in the spectra of free neomycin lies approximately at the same position in that of the neomycin complexes to suggest that the  $\text{NH}_2$  groups are not participating in coordination.

### 3.3 Electronic absorption spectra and magnetic susceptibility measurements:

From electronic spectra and magnetic moment data of the prepared complexes, Table 1, the structure and geometry of these complexes can be predicted, Figure 2. Vanadium, chromium, iron, cobalt and copper complexes are of octahedral geometry. Nickel, zinc and cadmium complexes are of tetrahedral geometry, but palladium complex is of square planar geometry.

#### 3.3.1 Vanadium- complex:

The nujol mull electronic absorption spectra of the dark green vanadium-complex showed three bands at 200, 450 and 800 nm due to  $2\text{B}_2\text{g} \rightarrow 2\text{E}_\text{g}$ ,  $2\text{B}_2\text{g} \rightarrow 2\text{B}_1\text{g}$  and  $2\text{B}_2\text{g} \rightarrow 2\text{A}_1\text{g}$  transitions, respectively. Its room temperature  $\mu_{\text{eff}}$  value of 4.21 B.M typified the existence of octahedral configuration [14]. The proposed structure depends on the bidentate nature of the organic compound with the presence of four water molecules in the inner sphere.

#### 3.3.2 Chromium- complex:

The nujol mull electronic absorption spectra for the pale green chromium complex showed three bands at 330 (s), 440 (w) and 610 (b) nm due to  $4\text{A}_2\text{g} \rightarrow 4\text{T}_2\text{g}$  (F),  $4\text{A}_2\text{g} \rightarrow 4\text{T}_1\text{g}$  (F) and  $4\text{A}_2\text{g} \rightarrow 4\text{T}_1\text{g}$  (P) transitions, respectively. So that this complex has octahedral geometry in high spin state. This complex has a magnetic moment of 5.12 B.M which is higher than the value expected for octahedral configuration due to the orbital contribute in the spin of the complexes. Furthermore, the high value of the  $\mu_{\text{eff}}$  of the complex points to a not purely octahedral geometry of the complex and a tendency to be distorted. The proposed structure of chromium complex was justified depending on bidentate nature of the organic compound through oxygen atoms of two OH alcoholic groups with the presence of four water molecules in the inner sphere [15].

#### 3.3.3 Iron- complex:

The nujol mull electronic absorption spectra of the dark brown iron-complex showed two bands at 390 (s) and 504 (b) due to  $\text{CT}(t_2\text{g} \rightarrow \pi^*)$  and  $\text{CT}(\pi \rightarrow \text{eg})$ , respectively. Its room temperature  $\mu_{\text{eff}}$  value of 5.92 B.M typified the existence of an octahedral configuration in high spin state [16], [17], [18].

#### 3.3.4 Cobalt- complex:

The nujol mull electronic absorption spectra of the rose cobalt-complex showed three bands at 360, 496 and 556 nm. The first band is due to metal to ligand charge transfer but the latter broad bands are due to  $4\text{T}_1\text{g}$  (F)  $\rightarrow 4\text{T}_1\text{g}$  (P) transition typified octahedral geometry. Its room temperature  $\mu_{\text{eff}}$  value of 5.03 B.M indicated high spin nature of the complex with three unpaired electrons and weak nature of the coordination bonds. The proposed structure of cobalt complex depends on bidentate

nature of the organic compound with the presence of one chloride ion and three water molecules in the inner sphere [19].

### 3.3.5 Nickel and palladium complexes:

The nujol mull electronic absorption spectra of the pale green nickel-complex showed two bands at 660 and 568 nm due to  $3T_1 \rightarrow 3T_2$  and  $3T_1 \rightarrow 3A_2$  transitions, respectively. Its room temperature  $\mu_{\text{eff}}$  value of 4.12 B.M typified the existence of the complex in tetrahedral geometry [20].

For diamagnetic palladium-complex,  $\mu_{\text{eff}} = \text{zero}$  to assign the low spin square planar configuration in which neomycin acts as a strong ligand. This complex showed two bands at (480,635 nm) which are assigned to ligand  $\rightarrow$  metal (L  $\rightarrow$  M) charge transfer so there are no d-d transitions. The structure of palladium-complex is based on bidentate nature of the organic compound, two water molecules in the inner sphere.

### 3.3.6 Copper- complex:

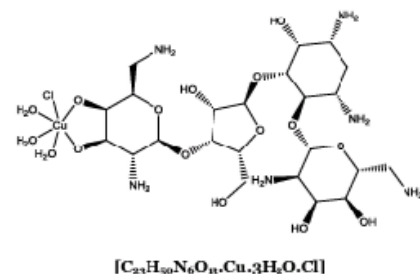
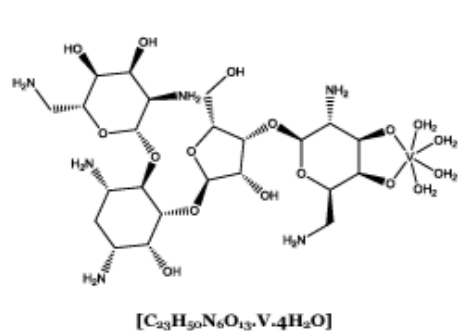
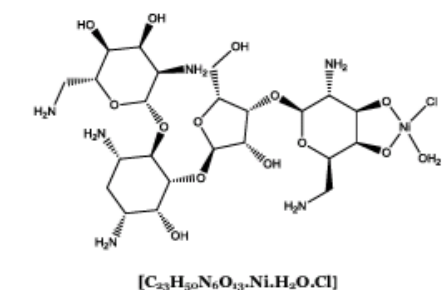
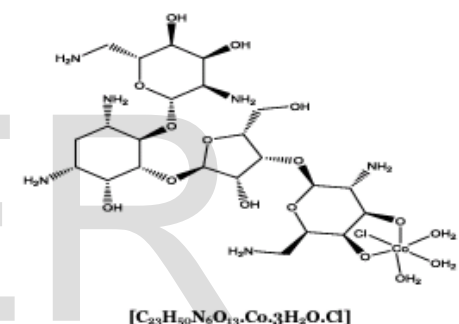
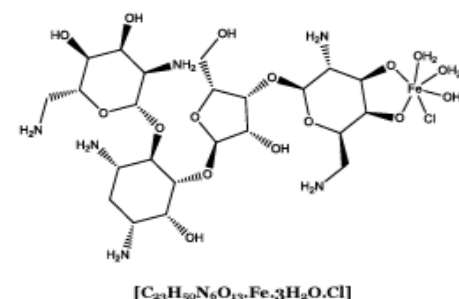
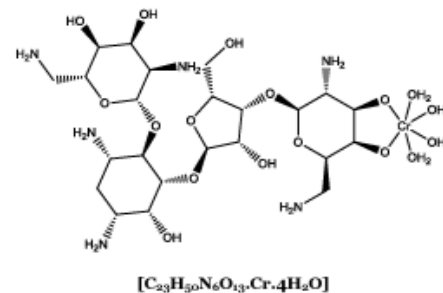
The nujol mull electronic absorption spectra of the dark blue copper-complex showed four bands at 400, 440, 600 and 734 nm. The first two bands are due to charge transfer but the two latter bands are due to  $2E \rightarrow 2T_2g$  (D) transition assignable to octahedral environment. Its room temperature  $\mu_{\text{eff}}$  value of 2.31 B.M which higher than the value corresponds to one unpaired electron 1.73 B.M due to the orbital contribute in the spin of the complexes. The proposed structure depends on the bidentate nature of the organic compound with the presence of one chloride ion and three water molecules in the inner sphere [21].

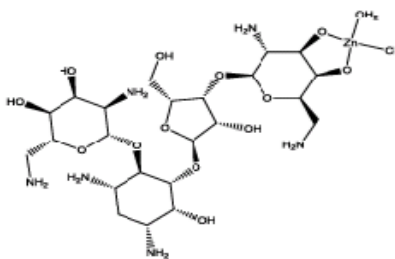
### 3.3.7 Zinc and cadmium complexes:

The nujol mull electronic absorption spectra of the pale yellow zinc and cadmium complexes showed two bands at (560,600 nm) and (500,610 nm) respectively, which are assigned to ligand metal (L  $\rightarrow$  M) charge transfer.

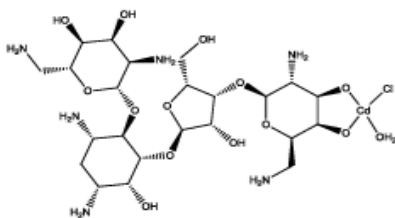
Owing to the  $d_{10}$ -configuration of Zn (II) and Cd (II), no d-d transition could be observed and therefore the stereochemistry around these metals in its complexes cannot be determined from ultraviolet and visible spectra ( $\mu_{\text{eff}} = \text{zero}$ ). However, by comparing the spectra of these complexes and those of similar environments, a tetrahedral geometry is suggested for these complexes [22].

The proposed structures for these complexes depend on the bidentate nature of the ligand through 2 oxygen atoms of 2 alcoholic OH groups with the presence of one chloride ion and one water molecule in the inner sphere.

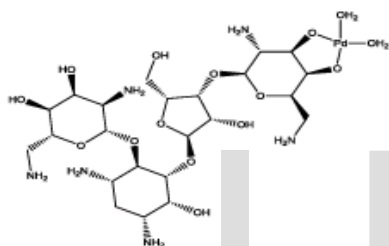




[C<sub>23</sub>H<sub>30</sub>N<sub>6</sub>O<sub>13</sub>·Zn·H<sub>2</sub>O·Cl]



[C<sub>23</sub>H<sub>30</sub>N<sub>6</sub>O<sub>13</sub>·Cd·H<sub>2</sub>O·Cl]



[C<sub>23</sub>H<sub>30</sub>N<sub>6</sub>O<sub>13</sub>·Pd·2H<sub>2</sub>O]

Fig. 2. Structures of Neomycin Metal Complexes.

### 3.4 Electron Spin Resonance (ESR) spectra for copper complex:-

The Cu (II)-neomycin complex exhibits an intense broad band consisting of three lines with no obvious hyperfine structure. The ESR spectrum of Cu (II)-neomycin complex showed an anisotropic spectrum of an axial-elongated octahedral type. It gave two g-values,  $g_{\parallel}=2.29$  and  $g_{\perp}=2.11$ , it is evident that unpaired electron is localized in the  $dx^2-y^2$  orbital and corresponds to square planar or elongated octahedral geometry of the complex, which is in reasonable agreement with the observed values of  $\lambda_{max}$  from electronic spectra of the copper complex which characteristic of elongated octahedral configuration [23].

The  $g_{av}$  ( $\langle g \rangle$ ) value is calculated from the relation:

$\langle g \rangle = (g_{\parallel} + 2g_{\perp}) / 3$  equal 2.17. The deviation of the  $\langle g \rangle$  value from that of the free electron (2.0023), suggests the high covalence property of complex with distorted Oh symmetry. In an axial environment, the exchange coupling interaction between the copper centers in polycrystalline sample is explained by the expression G-factor ( $G = (g_{\parallel} - 2.003) / (g_{\perp} - 2.003) = 4.0$ ). The exchange interaction is negligible if  $G > 4.0$ , where as a considerable interaction occurs for  $G < 4.0$ .

The calculated G value for Cu (II)-neomycin complex is 2.63 which is less than 4.0, indicates considerable exchange interaction in the solid complex [24].

### 3.5 Thermal Analysis:-

Thermal decomposition studies of neomycin, Figure 3. Figure 4. Figure 5, and some of its metal complexes have been carried out so as to corroborate the information obtained from their spectral about the status of water molecules present in these complexes as well as to know their general decomposition patterns. All complexes are decomposed in the same manner at three degradation steps.

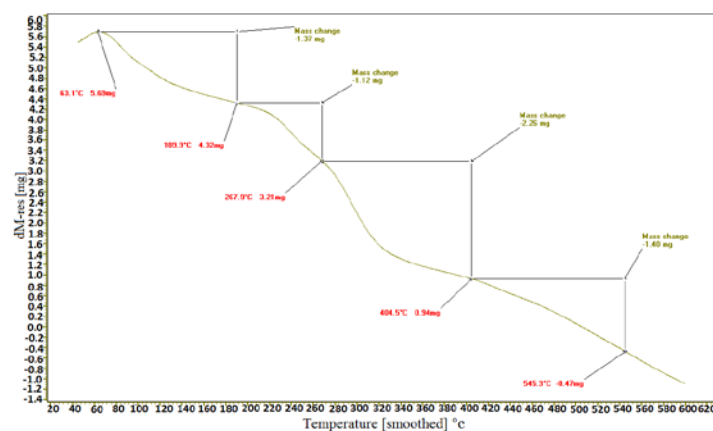


Fig. 3. TG Curve of Neomycin Sulphate.

First step from 60-220°C assigned to desolvation (loss of water of crystallization) as confirmed by the weight loss (%) obtained by the TG curve which corresponds to 4 water molecules in case of iron, copper, zinc and palladium complexes, 3 water molecules in case of vanadium complex and 5 water molecules in case of chromium complex.

Second step from 220-400°C assigned to a loss of 4 coordination water molecules in case of vanadium and chromium complexes, 3 in case of copper and iron complexes, 2 in case of palladium complex and 1 in case of zinc complex.

Third step from 400-600°C assigned to decomposition of complex and formation of metals oxide as a residue.

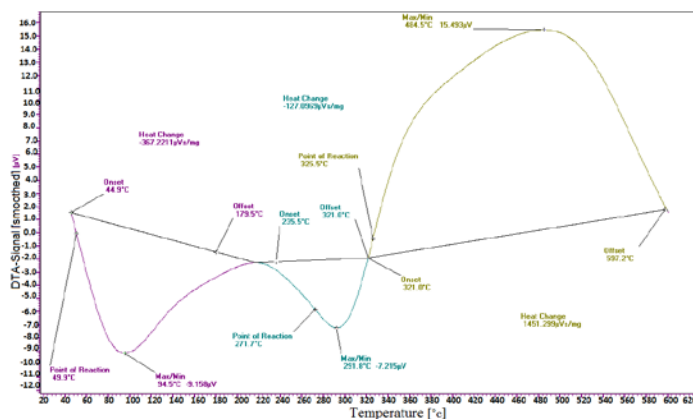
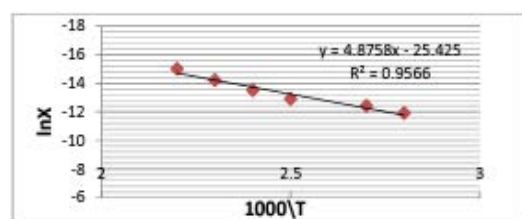


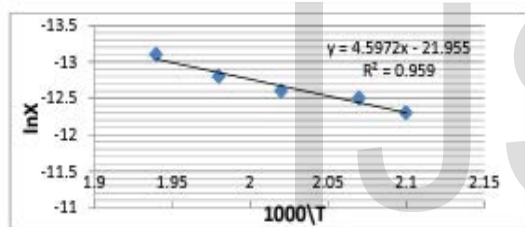
Fig. 4. DTA Curve of Neomycin Sulphate

The thermodynamic parameters of activation Table 2 can be calculated [25]. The negative value of the entropy of activation  $\Delta S^*$  of the decomposition steps of the metal complexes indicate that the activated fragments have more ordered structure than the undecomposed complexes and/or the decomposition reactions are slow [25].

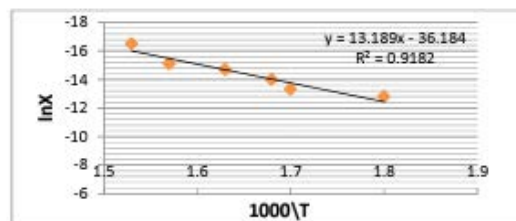
The positive sign of the enthalpy of activation  $\Delta H^*$  of the decomposition stages reveals that the decomposition steps are endothermic processes. The positive sign of free energy of activation  $\Delta G^*$  indicates that the free energy of the final residue is higher than that of the initial compound, and hence all the decomposition steps are nonspontaneous processes. Moreover, the values of  $\Delta G^*$  increase significantly for the subsequent decomposition stages of a given compound. The conclusion, as a result of the increasing of  $T\Delta S$ , reflects that the rate of removal of the subsequent species is lower than that of the precedent one [26], [27], [28].



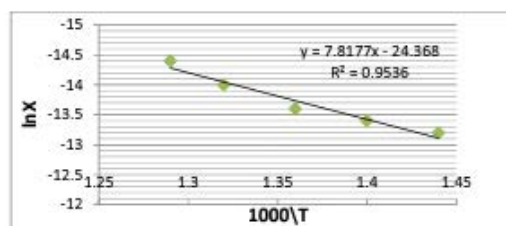
a) First degradation step.



b) Second degradation step.



c) Third degradation step.



d) Fourth degradation step.

Fig. 5. Coats-Redfern plots of four degradation steps for Neomycin Sulphate.

Differential scanning calorimetry (DSC) is also used to study the thermal transitions of a compound such as glass transition, melting and crystallization of the compound, Table 3 [29]. Differential scanning calorimetry studies of neomycin, Figure 6. Figure 7, and some of its metal complexes have been carried out.

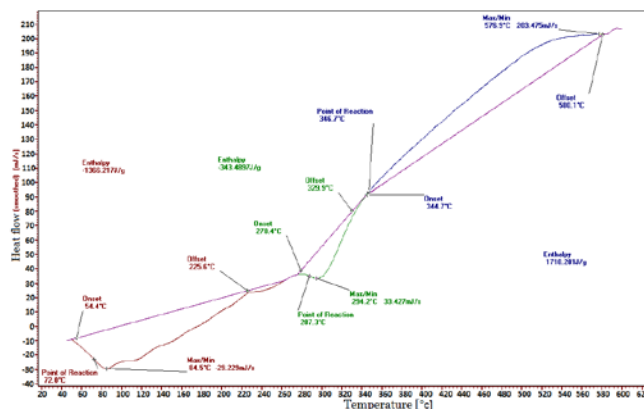


Fig. 6. DSC Curve of Neomycin Sulphate.

For the glass transition, there is no dip, and there's no peak because there is no latent heat given off, or absorbed, by the sample during the glass transition but there is a change in heat capacity. The glass transition called a second order transition. Both melting and crystallization involve giving off or absorbing heat so transitions like melting and crystallization are called first order transitions [30].

The glass transition temperature for complexes can be determined from DSC curve since they exhibit dehydration process due to coordinated water molecules followed by thermal agitation decomposition; this is compatible with the explanation of TG for these complexes. Vanadium neomycin complex has the highest value of  $T_g$  ( $107^\circ\text{C}$ ), while for the rest complexes,  $T_g$  is lowered to ranged between  $85\text{-}104^\circ\text{C}$ . The crystallization temperature of palladium complex is  $298^\circ\text{C}$  in which it will have gained enough energy to move into very ordered arrangements after that it gave off heat through an exothermic transition.

Palladium complex has the highest value of  $T_c$  while for the rest complexes  $T_c$  is lowered to range between  $98\text{-}295^\circ\text{C}$ .

All the prepared complexes melt above  $400^\circ\text{C}$ . DSC plot is used to carefully determine the melting temperature through an endothermic transition, where, the complexes should absorb heat until all the crystals have melted. Melting temperature of neomycin sulphate and its complexes are ranged between  $460\text{ to }629^\circ\text{C}$ .

However, the Debye model is applied to describe capacity change over a large temperature range; the  $C_p$  can be represented in the following empirical forms:

$$C_p = aT + b \quad \frac{C_p}{T} = \alpha T^2 + \gamma$$

By plotting  $C_p$  versus  $T$ , a straight line is obtained, where (a) & (b) parameters can be determined from the slope and intercept of the line, respectively. By plotting  $(C_p / T)$  versus  $T^2$ , a straight line is obtained, where (α) & (γ) are the

coefficients of electronic and lattice capacities, respectively Table 4 [31].  $C_p$  is the specific heat at constant pressure.

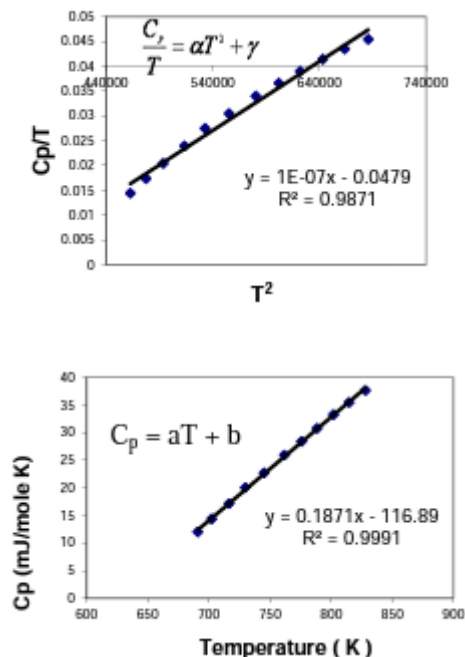


Fig. 7. Dependence of specific heat on temperature for Neomycin Sulphate.

TABLE 2: KINETIC PARAMETERS EVALUATED FOR NEOMYCIN SULPHATE AND ITS COMPLEXES.

Compound	Peak	Mid Temp.(K)	Ea (KJ/mol)	ΔH (KJ/mol)	ΔS (KJ/mol.K)	ΔG (KJ/mol)
C <sub>23</sub> H <sub>42</sub> N <sub>6</sub> O <sub>10</sub> ·3H <sub>2</sub> SO <sub>4</sub>	1 <sup>st</sup>	400	40.5	37.2	-0.220	125.1
	2 <sup>nd</sup>	502	38.2	34	-0.223	146.2
	3 <sup>rd</sup>	609	109.6	104.5	-0.221	239
[C <sub>23</sub> H <sub>40</sub> N <sub>6</sub> O <sub>10</sub> ·Cu <sub>3</sub> (H <sub>2</sub> O) <sub>2</sub> Cl](SO <sub>4</sub> ) <sub>3</sub> ·4H <sub>2</sub> O	1 <sup>st</sup>	412	33.6	30.2	-0.222	121.7
	2 <sup>nd</sup>	588	78.7	73.8	-0.222	204.5
	3 <sup>rd</sup>	777	37.8	31.3	-0.228	208.6
[C <sub>23</sub> H <sub>40</sub> N <sub>6</sub> O <sub>10</sub> ·Fe <sub>3</sub> (H <sub>2</sub> O) <sub>2</sub> Cl](SO <sub>4</sub> ) <sub>3</sub> ·4H <sub>2</sub> O	1 <sup>st</sup>	407	32.6	29.2	-0.222	119.4
	2 <sup>nd</sup>	566	70.4	65.7	-0.222	191.6
	3 <sup>rd</sup>	716	139.7	133.7	-0.222	292.7
[C <sub>23</sub> H <sub>40</sub> N <sub>6</sub> O <sub>10</sub> ·Zn <sub>3</sub> (H <sub>2</sub> O) <sub>2</sub> Cl](SO <sub>4</sub> ) <sub>3</sub> ·4H <sub>2</sub> O	1 <sup>st</sup>	419	27.5	23.9	-0.222	117.2
	2 <sup>nd</sup>	609	47.3	42.2	-0.225	179.1
	3 <sup>rd</sup>	816	36.7	29.9	-0.228	216.6
[C <sub>23</sub> H <sub>40</sub> N <sub>6</sub> O <sub>10</sub> ·Pd <sub>3</sub> (H <sub>2</sub> O) <sub>2</sub> Cl](SO <sub>4</sub> ) <sub>3</sub> ·4H <sub>2</sub> O	1 <sup>st</sup>	404	34.7	31.4	-0.221	120.7
	2 <sup>nd</sup>	488	42.5	38.5	-0.223	147.1
	3 <sup>rd</sup>	604	75.7	70.7	-0.224	206.1
[C <sub>23</sub> H <sub>40</sub> N <sub>6</sub> O <sub>10</sub> ·Cr <sub>3</sub> (H <sub>2</sub> O) <sub>2</sub> Cl](SO <sub>4</sub> ) <sub>3</sub> ·5H <sub>2</sub> O	1 <sup>st</sup>	404	34.7	31.4	-0.221	120.7
	2 <sup>nd</sup>	488	42.5	38.5	-0.223	147.1
	3 <sup>rd</sup>	604	75.7	70.7	-0.224	206.1
[C <sub>23</sub> H <sub>40</sub> N <sub>6</sub> O <sub>10</sub> ·V <sub>3</sub> (H <sub>2</sub> O) <sub>2</sub> Cl](SO <sub>4</sub> ) <sub>3</sub> ·3H <sub>2</sub> O	1 <sup>st</sup>	412	19.9	16.6	-0.223	108.5
	2 <sup>nd</sup>	569	48.2	46.5	-0.224	173.9
	3 <sup>rd</sup>	715	108.5	102.6	-0.223	262.1
	4 <sup>th</sup>	840	149.5	146.2	-0.224	334.2

TABLE 3: THERMAL TRANSITIONS OF NEOMYCIN SULPHATE AND SOME OF ITS COMPLEXES.

Compound	T <sub>g</sub> (°C)	T <sub>c</sub> (°C)	T <sub>m</sub> (°C)
Ligand	85	294	577
Cu-L complex	102	295	560
Fe-L complex	99	280	460
Zn-L complex	104	300	629
Pd-L complex	99	298	489
Cr-L complex	98	230	467
V-L complex	107	290	579

TABLE 4: THE SLOPES AND INTERCEPTS FOR DSC CURVES OF NEOMYCIN SULPHATE AND SOME OF ITS COMPLEXES.

Compound	C <sub>p</sub> = aT + b		$\frac{C_p}{T} = \alpha T^{-2} + \gamma$	
	a	b	$\alpha \times 10^{-7}$	$\gamma$
Ligand	0.187	-116.8	1	-0.047
Cu-L complex	0.032	-26.64	2×10 <sup>-1</sup>	-0.014
Fe-L complex	0.117	-77.9	1	-0.054
Zn-L complex	0.011	-7.895	8×10 <sup>-2</sup>	-0.003
Pd-L complex	0.07	-64.53	4×10 <sup>-1</sup>	-0.033
Cr-L complex	0.248	-200.5	2	-0.126
V-L complex	0.248	-200.5	2	-0.126

#### 4 MOLECULAR MODELING:-

Molecular modeling encompasses all theoretical methods and computational techniques used to model the behavior of molecules and their molecular structures [32], [33].

From molecular modeling data, neomycin, Figure 8, has several sites for coordination to different metal ions such as O(30), O(31), O(39), O(40), N(27), N(33), N(34) and N(35). These atoms carry charge values -0.429, -0.417, -0.448, -0.434, -0.262, -0.237, -0.305 and -0.286, respectively. Oxygen atoms of two alcoholic groups O(39) and O(40) carry more electronegative charge than other oxygen and nitrogen atoms confirming active sites for coordination.

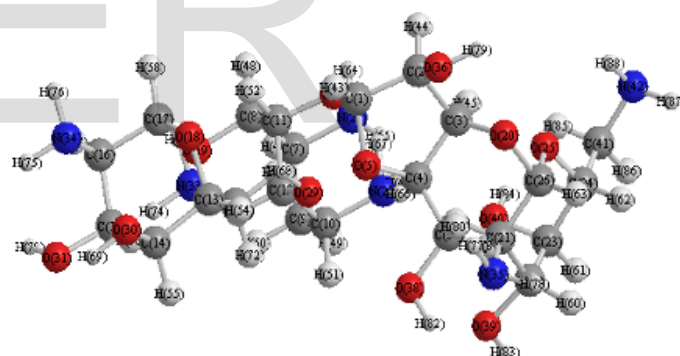


Fig. 8. Molecular modeling of Neomycin Sulphate

Comparing the bond lengths of C-C, C-N, C-O, C-H, N-H, and O-H atoms in free neomycin with that of its synthesized metal complexes, found that they are nearly equal (not affected by complexation), except bond lengths of C(22)-O(39) and C(23)-O(40) which become longer after complexation.

Thus, some of bonds show elongation upon complexation with the metal ions. From the analysis of the data calculated for the bond lengths, one can conclude that C(22)-O(39) and C(23)-O(40) bond lengths become longer in all complexes, as the coordination takes place via oxygen of the deprotonated hydroxyl groups. This finding is due to the formation of the M-O bond which makes the C-O bond weaker. Also, the long M-O bond in the complexes means that the ionic character of these bonds is small.

Most of bond angles for complexes are at  $\sim 120^\circ\text{C}$  and  $109.5^\circ\text{C}$ , this leads to suggest that most of the configurations are with  $sp^2$  and  $sp^3$ - hybridization, respectively. The deviation appeared in the region of complexation between metal and oxygen atoms of two alcoholic groups and also between metal and oxygen atoms of coordinated water molecules for O(46)-M(43)-O(45), O(46)-M(43)-O(39), O(46)-M(43)-O(40), O(39)-M(43)-O(40) and O(47)-M(43)-O(45) which are equal to  $90, 90, 90, 80.15$  and  $34.48^\circ\text{C}$ , respectively, where  $M = \text{Fe, Cu, Co, V}$  and  $\text{Cr}$  atoms. The decrease of the bond angles on complexation is due to the presence of metal between two higher electronegative oxygen atoms.

The bond lengths between iron, copper, cobalt and nickel atoms with chloride atom are nearly equal to ( $2.16 \text{ \AA}$ ), which are longer than bond length between these metals with oxygen atoms which are nearly equal to ( $1.81 \text{ \AA}$ ), due to higher electronegativity of oxygen than chloride.

The bond lengths between Fe(43), Cu(43), Zn(43), Ni(43), Co(43), V(43), Cr(43) and Pd (43) with all oxygen atoms are equal. But the bond length between Cd(43) with O(40) and O(39) atoms inside the ring ( $2.12 \text{ \AA}$ ) is greater than bond length between Cd(43) and O(45) atom outside the ring ( $1.95 \text{ \AA}$ ).

The bond length between zinc and chloride atoms ( $2.24 \text{ \AA}$ ) is longer than that of zinc and oxygen atoms ( $1.89 \text{ \AA}$ ) due to higher electronegativity of oxygen than chloride. Similar situation is recorded for bond length between cadmium and chloride atoms ( $2.47 \text{ \AA}$ ) which also longer than that of cadmium and oxygen atoms ( $2.12 \text{ \AA}$ ).

The lowest value of the bond length is observed in case of O-H ( $0.942 \text{ \AA}$ ), while the highest value is in case of metal-chloride bonds. The bond angles of O-M-O and O-M-Cl which are nearly equal to  $90^\circ$ , where  $M = \text{Fe, Cu, Co, V}$  and  $\text{Cr}$  atoms, indicates octahedral structure.

Positive and negative signs of dihedral angles of the ligand and its metal complexes indicate that atoms are located in plane or out of plane. It seems that, in some cases, the dihedral angle of zero is attributed that the orientation and the distribution of the atoms are of different environments, i.e. parallel, antiparallel leading to zero values.

Quantum chemical parameters such as the highest occupied molecular orbital energy (EHOMO), the lowest unoccupied molecular orbital energy (ELUMO), energy gap ( $\Delta E$ ) and parameters which give information about the reactive behavior of compounds such as electronegativity ( $\chi$ ), chemical potential ( $\mu$ ), global hardness ( $\eta$ ), softness ( $\sigma$ ) and electrophilicity index ( $\omega$ ) [34], [35], [36], [37] were calculated, Table 5.

The higher EHOMO value of neomycin sulphate, the easier it's offering electrons to the unoccupied d-orbital of the transition metals center and the greater its ability to complexation.

Also, the EHOMO and ELUMO have negative signs, which indicate that the compound is stable. Neomycin has a large energy gap ( $\Delta E$ ) and also has a high global hardness value, so it is considered as a hard molecule.

TABLE 5: QUANTUM CHEMICAL PARAMETERS (EV) OF THE NEOMYCIN SULPHATE CALCULATED BY PM3 METHOD.

Compound	EHOMO (E <sub>H</sub> )	ELUMO (E <sub>L</sub> )	$\Delta E = (E_L - E_H)$	$\chi$	$\mu$	$\eta$	$\sigma$	$\omega$
Neomycin sulphate	-8.209	-0.628	7.581	4.418	-4.418	3.791	0.264	2.575

## 5 BIOLOGICAL ACTIVITY:-

### 5.1 Antimicrobial examination:

Many metal complexes have powerful antimicrobial activities and some of them are already in market such as silver bandages for treatment of burns. The discovery and development of effective antibacterial and antifungal drugs with novel mechanism of action has become an urgent task for infectious disease [38].

The antimicrobial screening of the ligand and some of its synthesized complexes data, Table 6. All samples showed good results with mean zone of inhibition values less than used standards Amphotericin B as antifungi, Ampicillin as anti-gram positive bacteria and Gentamicin as anti-gram negative bacteria.

Copper and Palladium complexes showed more antifungal activities against *Aspergillus fumigatus* than free ligand but Iron and Zinc complexes showed less antifungal activities than free ligand, while all tested compounds showed no activity against *Candida albicans*. In addition, all synthesized complexes showed more anti-gram positive bacterial effect against *Streptococcus pneumoniae* and *Bacillus subtilis* than free ligand.

All synthesized complexes showed more anti-gram negative bacterial effect against *Escherichia coli* than free ligand except Zinc complex that showed less anti-gram negative bacterial effect than free ligand, while all tested compounds showed no activity against *Pseudomonas aeruginosa*.

The obtained data confirmed that Palladium complex was the most antifungal effective compound against *Aspergillus fumigatus* and an excellent anti-gram positive bacterial effect on both *Streptococcus pneumoniae* and *Bacillus subtilis* compared to other examined compounds. In addition Palladium complex showed a good anti-gram negative bacterial effect on *Escherichia coli* compared to other examined compounds.

Based on these results, complex formation tends to make the ligand acts as more powerful and potent anti-bacterial and antifungal agent, except Iron and Zinc complexes against *Aspergillus fumigatus* tends to decrease the antifungal activity of the ligand, also Zinc complex against *Escherichia coli* tends to decrease the anti-gram negative bacterial activity of the ligand.

A possible explanation for increase the activity upon chelation is that, in chelated complex, positive charge of the metal is partially shared with donor atoms present on ligands and there is an electron delocalization over the whole chelating ring. This may increase the lipophilicity of the bacterial membranes [39].



The cell permeability depends on the lipid membrane that surrounds the cell which favours the passage of only lipid soluble materials on the basis that liposolubility is an important factor that controls antimicrobial activity. On chelation, the polarity of the metal ion is reduced to a greater extent to the overlap of the ligand orbital and partial sharing of the positive charge of the metal ion with the donor groups. Further, it increases the delocalization of p- and d- electrons over the whole chelate and enhances the lipophilicity of the complex; the increased lipophilicity enhances the penetration of the complexes into lipid membranes and blocking of metal binding sites on the enzymes of the microorganisms [39].

TABLE 6: ANTIBACTERIAL AND ANTIFUNGAL ACTIVITIES OF SOME SYNTHESIZED COMPLEXES.

Microorganism compound	Mean zone of inhibition in mm ± S.D.					
	<i>Aspergillus fumigates</i>	<i>Candida albicans</i>	<i>Streptococcus pneumoniae</i>	<i>Bacillus subtilis</i>	<i>Pseudomonas aeruginosa</i>	<i>Escherichia coli</i>
L	14.3 ± 0.86	NA	12.2 ± 0.72	13.6 ± 0.63	NA	11.4 ± 1.5
Cu-L	17.4 ± 1.2	NA	18.1 ± 1.2	18.9 ± 0.25	NA	16.1 ± 0.72
Fe-L	11.4 ± 0.63	NA	15.2 ± 0.72	15.9 ± 0.58	NA	12.1 ± 0.58
Zn-L	13.4 ± 0.72	NA	14.2 ± 0.63	15.1 ± 0.58	NA	11.0 ± 1.2
Pd-L	18.2 ± 0.58	NA	19.6 ± 0.63	20.1 ± 0.72	NA	16.48 ± 0.72
Amphotericin B	23.8 ± 0.58	24.3 ± 0.63	-----	-----	-----	-----
Ampicillin	-----	-----	22.5 ± 1.2	29.8 ± 0.58	-----	-----
Gentamicin	-----	-----	-----	-----	19.4 ± 1.2	20.6 ± 0.63

Where, NA: no activity.  
Amphotericin B: Standard for fungi.  
Ampicillin: Standard for gram-positive bacteria.  
Gentamicin: Standard for gram-negative bacteria.

### 5.2 Antioxidant property:

Free radicals, which are generated in several biochemical reactions in the body, have been implicated as mediators of many diseases, including cancer, atherosclerosis and heart diseases [40], [41].

The obtained results showed that all examined compounds have scavenging activity to the DPPH free radicals, with different values regarding to their distinct structures, compared to vitamin E as an antioxidant reference.

The effective concentration of sample required to scavenge DPPH radical by 50% (EC50 value) was obtained by linear regression analysis of dose-response curve plotting between %scavenging and concentrations.

Moreover, the calculated EC50 of Cu-neomycin, Pd-neomycin and Zn-neomycin complexes were found to be: 0.38, 0.39 and 0.45 respectively, indicated that these compounds have the highest scavenging activity and the highest antioxidant effect, especially Cu-neomycin complex which has the lowest EC50 value so it has highest scavenging activity and the highest antioxidant effect, Figure 9 and Table 7.

The obtained results from antimicrobial and antioxidant examinations showed that copper and palladium complexes have the highest antioxidant and antimicrobial effects.

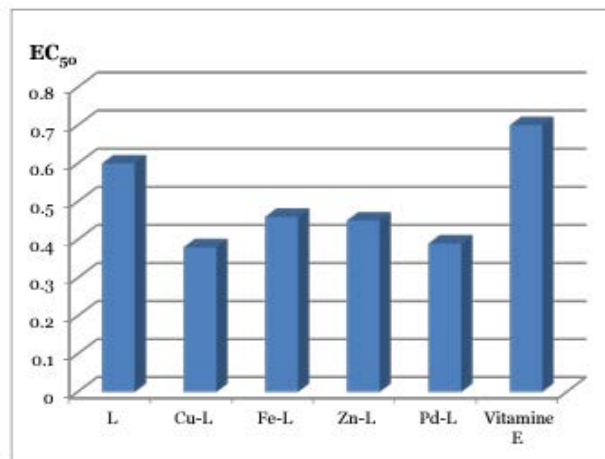


Fig. 9. EC50 values for Neomycin Sulphate ligand and its complexes compared to Vitamine E as standard.

Copper complex has higher antioxidant and antimicrobial effects than iron complex as octahedral complexes, but square planer palladium complex has higher antioxidant and antimicrobial effects than tetrahedral zinc complex.

The trend of decreasing the biological activity of complexes is palladium (square planer), copper (octahedral), iron (octahedral) and zinc (tetrahedral). Accordingly, the antimicrobial activity and the antioxidant property of these complexes seem to be highly affected by their structural geometries where, square planer complexes possess higher antimicrobial and antioxidant activities than octahedral complexes than tetrahedral complexes.

From the molecular modeling results, the value of charge on palladium atom is higher than copper, iron and zinc atoms, so the biological activity of complexes is directly proportional to the value of charge on metal atom which participates in coordination. Compounds with noticeable activity may be considered as a start point for development of some new antimicrobial and antioxidant agents.

TABLE 7: EC50 VALUE FOR NEOMYCIN SULPHATE AND ITS COMPLEXES COMPARED TO VITAMINE E AS STANDARD.

Compound	EC50
L	0.6
Cu-L	0.38
Fe-L	0.46
Zn-L	0.45
Pd-L	0.39
Vitamine E	0.7

Where, L: Ligand, Cu-L: Copper complex, Fe-L: Iron complex, Zn-L: Zinc complex and Pd-L: Palladium complex.

## 6 CONCLUSION:-

A series of transition metals neomycin complexes having the formula  $[M(\text{Neom})(\text{H}_2\text{O})_m \text{Cl}_n] \cdot x\text{H}_2\text{O} \cdot 3\text{SO}_4$  were prepared. IR spectra indicated that the bonding between neomycin and transition metal ions takes place through M-O bonds. Neomycin can react with metal ions as dianionic bidentate ligand through  $\text{H}^+$  ion displacement from 2 OH alcoholic groups. The prepared transition metal neomycin sulphate complexes were found to have different properties, spectral and different biological activities of neomycin itself.

Biological screening for neomycin and some of its synthesized complexes involving antimicrobial (antibacterial, antifungal) and antioxidant were done. These examinations showed that complexes have higher antioxidant and antimicrobial effects than neomycin itself. From the molecular modeling results, the value of charge on palladium atom is higher than copper, iron and zinc atoms, so the biological activity of complexes is directly proportional to the value of charge on metal atom which participates in coordination. Compounds with noticeable activity may be considered as a start point for development of some new antimicrobial and antioxidant agents.

## 7 REFERENCES

- [1] Ming, L. J. Structure and function of metalloantibiotics, Med. Res. Rev. Wiley Online Library 2003, 23(6), 697-762.
- [2] Warra, A. A. "Transition metal complexes and their application in drugs and cosmetics", J. Chem. Pharm. Res 2011, 3(4), 951-958.
- [3] Hoffman, L. R. ; D'Argenio, D. A.; MacCoss, M. J.; Zhang, Z.; Jones R. A. and Miller, S. L, Aminoglycoside antibiotics induce bacterial biofilm formation 2005, 436 (25), 1171.
- [4] Cammack, R.; Atwood, T. K.; Campbell, P. N.; Parish, J. H.; Smith, A. D.; Stirling J. L. and Vella, F. "Oxford Dictionary of Biochemistry and Molecular Biology (2nd Edition) - neomycin." Oxford University Press. 2006, 453.
- [5] Kiyoshi, T. and Robertson, J. H. "Comparative Study of Responses to Neomycins B and C by Microbiological and Gas-Liquid Chromatographic Assay Methods." Applied Microbiology 1969, 18(3), 396-98.
- [6] Abu-El-Wafa, S. M. ; El-Ries, M. A. ; Abou-attia F. M. and Issa R. M.; Coordination Chemical Studies of Some Polymeric Transition Metal Complexes with Neomycin and Their Biological Activity Uses. Indirect Determination of Neomycin by Atomic Absorption Spectroscopy (AAS), Analytical Letters, 1989, 22(13-14), 2703-2716.
- [7] Schwarzenbach, G. "Complexometric Titration", translated by H. Irving. Methuen Co., London (1957).
- [8] Masoud, M. S.; Abou El-Enein, S. A. and Obeid, N. A. , Electronic spectral properties of some substituted arylazothio barbiturate compounds in presence of different solvents Z. Fur Phys. Chem, 2001, 215(7), 867-881.
- [9] Figgis, B. N. and Lewis, J., Modern coordination chemistry, New York, (1967) P. 403.
- [10] Hindler, J. A.; Howard B. J. and Keiser J. F., Antimicrobial agents and susceptibility testing in: B. J. Howard, Clinical and pathogenic Microbiology, Mosby- year Book Inc. St. Louis, MO, USA (1994).
- [11] Williams, W. B. ; cuvelier, M. E. and Berset, C., Use of a free radical method to evaluate antioxidant activity. Lebenson Wiss Technol 1995, 28, 25-30.
- [12] Hamid, A. A. ; Aiyelaagbe, O. O.; Usman, L. A. ; Ameen, O. M. and Lawal, A. "Antioxidants: Its medicinal and pharmacological applications.", 2010, 4(8), 142-151.
- [13] Nakamoto, K. "Infrared Spectra of Inorganic and coordination compounds". John Wiley N. Y. (1977).
- [14] Swamy, S. J.; Reddy A.D.; and Bhaskar, K.; Synthesis and spectral studies of some oxovanadium(IV) and vanadium(IV) complexes, Indian J. of Chem., 2001, 40, 1166-1171.
- [15] Price E. R. and Wasson, J. R. ; Complexes with sulfur and selenium donors -x chromium (III) piperidylthiocarbamates, J. Inorg. Nucl. Chem, 1974, 36(1), 67-71.
- [16] Barefield, E. K. ; Busch D. H. and Nelson, S. M. ; Iron, cobalt and nickel complexes having anomalous magnetic moments, Quart. Rev, 1968, 22(4), 457-498.
- [17] Barnum, D. W. ; Electronic absorption spectra of acetylacetonato complexes- II: Huckel LCAO-MO calculations for complexes with trivalent transition metal ions J. Inorg. Nucl. Chem, 1961, 22(4), 183-191.
- [18] Singh A. and Singh, P. ; Synthesis, characterization and anti-inflammatory effects of Cr (III), Mn (II), Fe (III) and Zn (II) complexes with diclofenac sodium, Ind. J. Chem., 2000, 39A, 874-876.
- [19] Lever, A. B. P. "Inorganic Electronic Spectroscopy", Elsevier publish Co, Amsterdam, 1968.
- [20] Nelson, S. N. and Sheperd, T. M.; The coordination number of transition metal ions. Part III. Complexes of nickel (II) halides with heterocyclic aromatic amines, J. Chem. Soc, 1965, 3276-3284.
- [21] Atkins, R.; Brewer, G.; Kokot, E.; Mockler G. M. and Sinn, E.; Copper(II) and Nickel(II) Complexes of some Unsymmetrical tetradentate Schiff Base Ligands. Inorg. Chem, 1985, 24, 127-134.
- [22] Jeeva, J. and Ramachandramoorthy, T. ; Microwave Assisted Synthesis and Characterisation of Diamagnetic Complexes. Research Journal of Chemical Sciences; 2013, 3(9): 69-76.
- [23] Bhoon, Y. K. "Magnetic and EPR properties of Mn(II), Fe(III), Ni(II) and Cu(II) complexes of thiosemicarbazone of  $\alpha$ -hydroxy- $\beta$ -naphthaldehyde", Elsevier; 1983, 2: 365-368.
- [24] Dutta, R. L. ; Syamal, A.; Elements of Magnetochemistry, Affiliated East West Press Pvt Ltd. Prabhugouda (1993).
- [25] Frost, A. A. and Pearson, R. G. ; "Kinetics and Mechanisms", Wiley, New-York (1961).
- [26] Maravalli, P. B. and Goudar, T. R. ; Thermochemico Acta; 1999, 235, 35-42.
- [27] Yusuff, K. K. M. and Sreekala, R. ; "Thermal decomposition kinetics of iron(III), cobalt(III), nickel(II) and copper(II) complexes of a Schiff base derived from quinoxaline-2-carboxaldehyde and glycine", Reaction Kinetics and Catalysis Letters; 1992, 48(2): 575-581.
- [28] Kandil, S. S.; El-Hefnawy, G. B. and Baker, E. A. ; Thermochemico Acta; 2004, 414: 105.
- [29] Elder, J. P.; Multiple reaction scheme modeling, J. Thermal Anal., 1990, 36: 1077-1112.
- [30] Hatakeyama T. and Zhenhalliu "Wiley-Hand book of thermal analysis" 72 (1999).
- [31] Toda, A.; Tomita, C. ; Hikosaka, M. and Saruyama, Y.; Kinetics of irreversible melting of polyethylene crystals revealed by temperature modulated DSC, Thermochem. Acta, 1998, 324 (1-2), 95-107.
- [32] Frenkel, D. and Smit, B.; " Understanding molecular simulation: From algorithms to applications", ISBN 0-12-267370-0 (1996).
- [33] Leach, A. R. ; "Molecular modeling: principles and applications", ISBN 0-582-38210-6 (2001).
- [34] Laarej, K. ; Bouachrine, M.; Radi, S.; Kertit S. and Hammouti, B.; Quantum chemical studies on the inhibiting effect of bipyrazoles on steel corrosion in HCL, E. J. Chem., 2010, 7(2), 419-424.
- [35] Pearson, R. G.; Absolute electronegativity and hardness: applications to organic chemistry, J. Org. Chem., 1989, 54(6), 1423-1430.
- [36] Baetzold, R. C.; Atomistic modeling of silver clusters formed on the surface of AgBr, J. Phys. Chem., 2007, 111(3), 1385-1391.
- [37] Masoud, M. S. ; Ali, A. E. ; Shaker, M. A. and Elsalala, G. S. ; Synthesis, computational, spectroscopic, thermal and antimicrobial activity studies on some metal-urate complexes, Spectrochim. Acta A., 2012, 90(1), 93-108.
- [38] Jayaseelan, P.; Prasad, S.; Vedanayaki, S. and Rajavel, R.; Synthesis, Spectral Characterization, Thermal and Anti-microbial Studies of New Binuclear Metal Complexes Containing Tetradentate Schiff Base Ligand, Int. J. Chem. Environ. Pharm. Res. 2010, 1(2), 80-88.
- [39] Anacona, J. R. ; Brito, L. and Pena, W. ; Synthesis and reactivity in inorganic,

Metal-Organic & Nano-Metal Chem, 2012, 42, 1278-1284.

- [40] Hayet, E. ; Maha, M.; Samia, A.; Mata, M.; Gros, P.; Raida, H; Ali, M. M. ;Mohamed, A. S.; Gutmann, L.; Mighri, Z. and Mahjoub, A.; World J. Microbiol. Biotechnol. 2008, 24, 2933.
- [41] Sies, H; "Oxidative stress: oxidants and antioxidants." Exp Physiol, 1997, 82(2), 291-295.

IJSER